Performance of a novel Sn-Ag-Cu-Pt solder as interconnections in bi-facial solar cells under the sun

Chin Kim **Lo**[*1], Karen Mee Chu **Wong**[1], Yun Seng **Lim**[1], Yee Kai **Tian**[1]

[1]Faculty of Engineering and Science, Universiti Tunku Abdul Rahman,

Jalan Genting Klang, 53300, Kuala Lumpur, Malaysia

[*]Corresponding author's phone: +603-41079802

E-mail: ukwn.cklo@gmail.com

Date Received 14th June 2013
Date Revised 27th November 2013
Date Accepted 3rd December 2013

ABSTRACT

The performance of a solar panel is expected to be improved by using a low resistivity solder in the interconnection of bi-facial solar cells. Two solar panels were constructed using the popular Sn-3.8Ag-0.7Cu solder and a new Sn-3.8Ag-0.7Cu-0.2Pt composite solder as interconnection material. The power outputs of both solar panels under the sun were measured constantly throughout one week using an IV plotter and the total energy yields were calculated and compared. The total energy yield increases by 9.68% for the solar panel with the new Sn-Ag-Cu-Pt composite solder compared to that with the conventional Sn-Ag-Cu solder. This provides an alternative approach to boost the solar panel performance. Both solar panels have almost the same maximum power output throughout the week showing that the new solder is stable and shows no sign of degradation under the sun.

Keywords: Bi-facial solar cell, Composite solder, Interconnection, Power output

1.0 INTRODUCTION

Bi-facial solar cell, unlike ordinary solar cells, is able to absorb sunlight from both sides to generate electricity. A number of bi-facial solar cells are connected together by soldering to form a bi-facial solar panel.

Soldering is the most common and important way to connect the solar cell due to their excellent electrical conductivity, wetting behaviour and low melting temperature [1–5]. Therefore, solar panel interconnection materials are important due to their significant effects on energy production efficiency and reliability in real applications [6,7]. Previously, lead-based Sn-Pb (Tin-Lead) solder was widely used in electronic packaging due to some of its technical advantages, such as low melting point, outstanding wetting and spreading capabilities, competitive cost, satisfactory strength, ductility, and fatigue resistance [2,8–12]. However, the use of Sn-Pb was restricted due to environmental and toxicological concerns associated with the material [13]. As such, lead-free solder is the preferable choice in green technology.

Among the lead-free solders such as Sn-Ag (Tin-Silver), Sn-Cu (Tin-Copper), Sn-Zn (Tin-Zinc), Sn-Ag-Cu (Tin-Silver-Copper), etc., Sn-Ag-Cu was regarded as the most promising lead-free solder due to its good mechanical properties, acceptable wetting properties as well as suitable melting points [12,14–17]. The main issue impeding the successful application of all lead-free solders is the formation of excessive intermetallic compounds (IMC) between the solder and base material [8,18,19], resulting in various connectivity and reliability problems. Alloying elements such as Ni (Nickel), Ag (Silver), Pt (Platinum), Al (Aluminium), Co (Cobalt), Bi (Bismuth), rare earth elements, etc. had been added into the lead-free solders to enhance the properties of the interconnection. Among these, Pt possess several good properties such as low dissolution rate and resistance to oxidation [20,21]. The Sn-Ag-Cu-Pt solder was

developed to suppress excessive IMC growth. The objective of this study is to investigate the performance of Sn-Ag-Cu-Pt composite solder in bifacial solar cells under the actual operational condition.

In this study a newly developed Sn-Ag-Cu-Pt composite solder alloy was used in the interconnection of bi-facial solar cells. The interconnected solar cells that formed a bi-facial solar panel were placed under the sun to measure its performance and to calculate the contact resistance. The result was then compared with that of the bi-facial solar cells connected by conventional Sn-Ag-Cu solder.

2.0 MATERIALS AND METHODS

Bi-facial solar cells (Figure 1) were purchased from PVG Solutions and connected to form two solar panels using the two types of solder, the novel Sn-3.8Ag-0.7Cu-0.2Pt composite solder and the conventional Sn-3.8Ag-0.7Cu solder, as shown in Figure 2. Agilent N3300A electronic load with two units of N3305A electronic load modules were used to carry out the solar panels electrical output measurement. The electronic load was controlled and programmed by an IV plotter program created in Agilent VEE programming environment. Flow chart for measurement of the power output is shown in Figure 3.

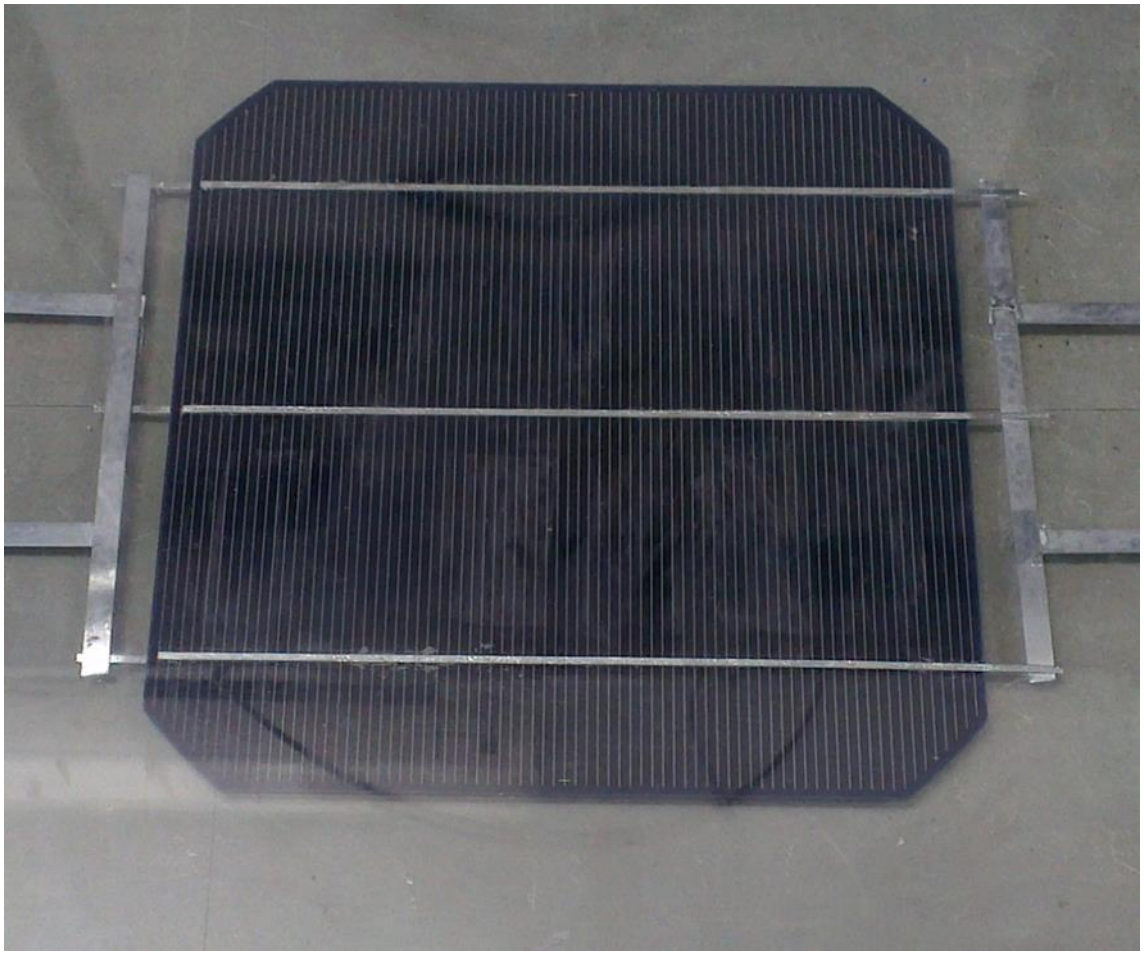

Figure 1: A bi-facial solar cell

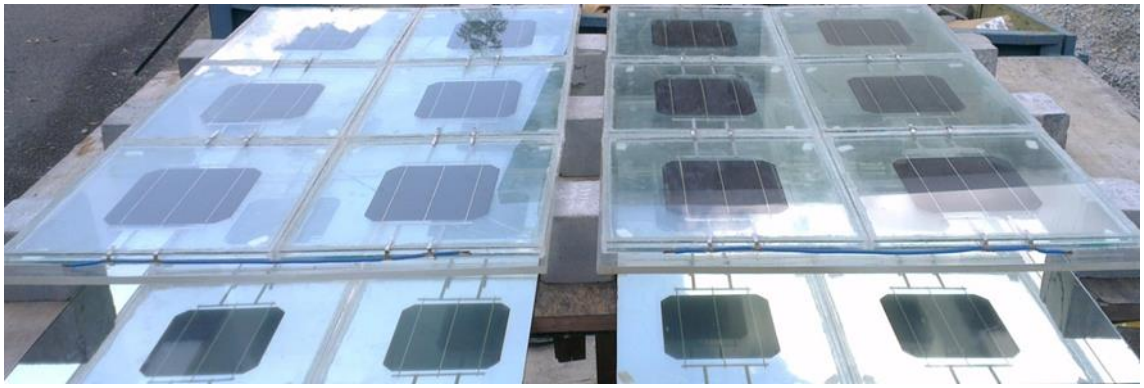

Figure 2: Bi-facial solar panels

Identical soldering process was used in the manufacturing process of the both solar panels using Sn-Ag-Cu solder and Sn-Ag-Cu-Pt solder. The solar panels were placed side by side under the sun at Universiti Tunku Abdul Rahman, Kuala Lumpur, Malaysia. The solar panel installation location has a mean temperature of 29°C and average humidity of 82% throughout the duration of the experiment. Both solar panels were connected to an electronic load for measurement of electrical output. An IV plotter program (Figure 4) was written for the electronic load to vary the resistive loads connected to the solar panels and measure both voltage and current simultaneously from both solar panels. The current-voltage graphs and power-voltage graphs were then plotted by the program to determine the power outputs from both solar panels. The electrical output measurement was taken at scheduled intervals between 10am to 4pm over a period of seven continuous non-rainy days.

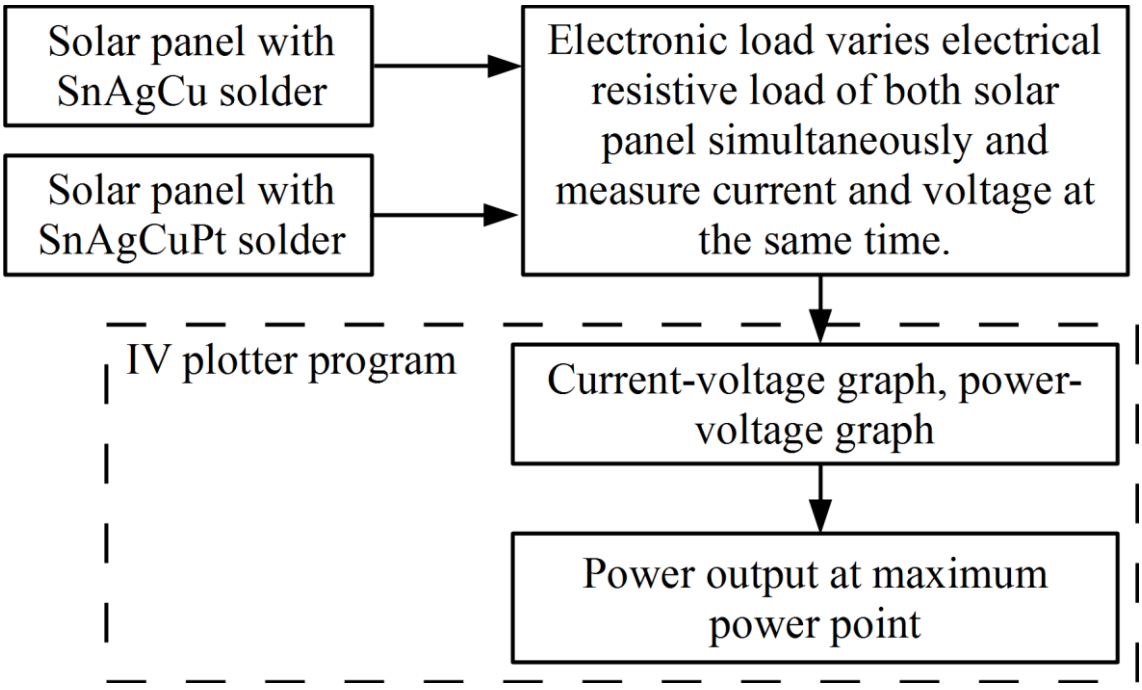

Figure 3: Flow chart of the power output measurement

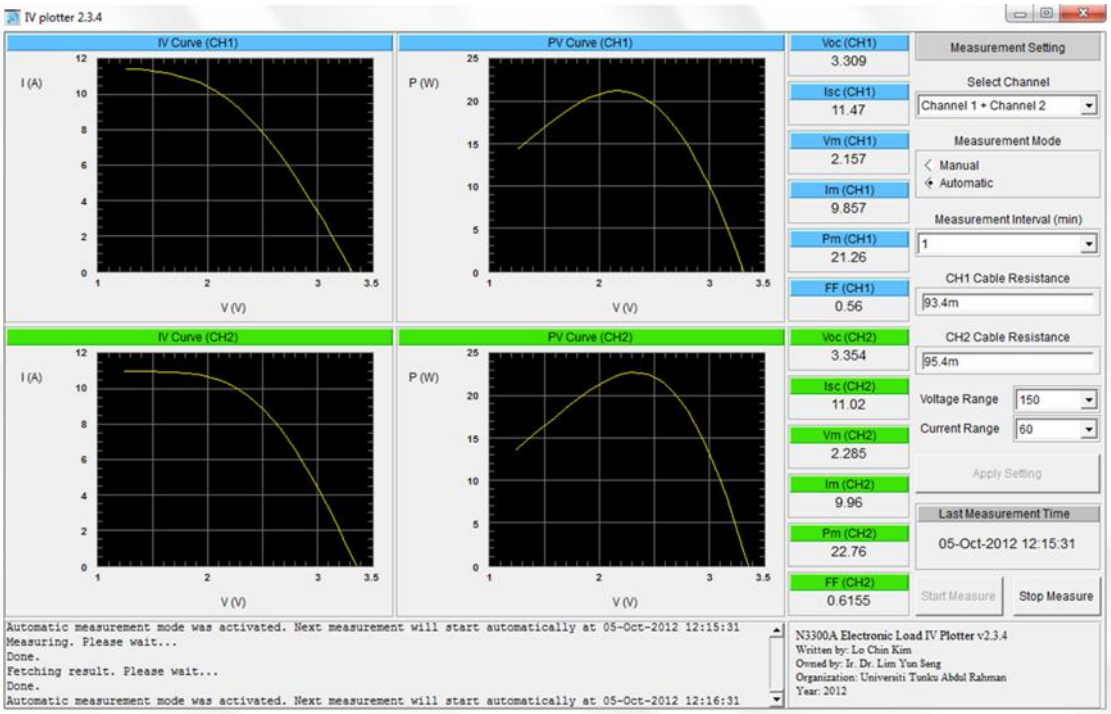

Figure 4: Screenshot of the IV plotter program

During the measurement, sunlight intensity varied from time to time. The electronic load was programmed to record the required voltage and current measurement from both solar panels simultaneously within one second. This ensures that the current-voltage and power-voltage graphs are plotted fast enough without being affected by the variation in sunlight intensity.

Power output values at maximum power points from both solar panels, taken throughout one day were used to calculate the daily energy yields from the solar panels. The daily energy yield from a solar panel was calculated by integrating the power output of a solar panel with respect to time throughout the day.

Besides, the current-voltage graph was curve-fitted using Equation (1) to extract the series resistance, R_s. Equation (1) is the circuit equation of the solar cell single diode model as shown in Figure 5.

$$I = I_{ph} - I_0\left[\exp\left(\frac{V + IR_s}{AV_T}\right) - 1\right] - \frac{V + IR_s}{R_{sh}} \qquad \text{- Equation (1)}$$

Where,
I = Measured solar cell current (A);
V = Measured solar cell voltage (V);
I_{ph} = Photogenerated current (A);
I_0 = Reverse saturation current (A);
R_s = Series resistance (Ω);
R_{sh} = Shunt resistance (Ω);
A = Diode ideality factor;
V_T = Thermal voltage (V) = kT/q;
k = Boltzmann constant (eV/K);
T = Solar cell temperature (K);
q = Elementary charge constant (C).

All the recorded current-voltage data throughout the seven-day period were curve-fitted in MATLAB. However, only those with good fit or R^2 values equals or greater than 0.9999 were plotted into the result. The difference in series resistance from two solar panels is given by the difference in the solder resistance as both panels are identical except for the different types of solders used in each. Therefore, the change in solder resistance was represented by the difference of series resistances from the two solar panels. The increase in daily yield and decrease in solder resistance over the seven-day period can then be computed.

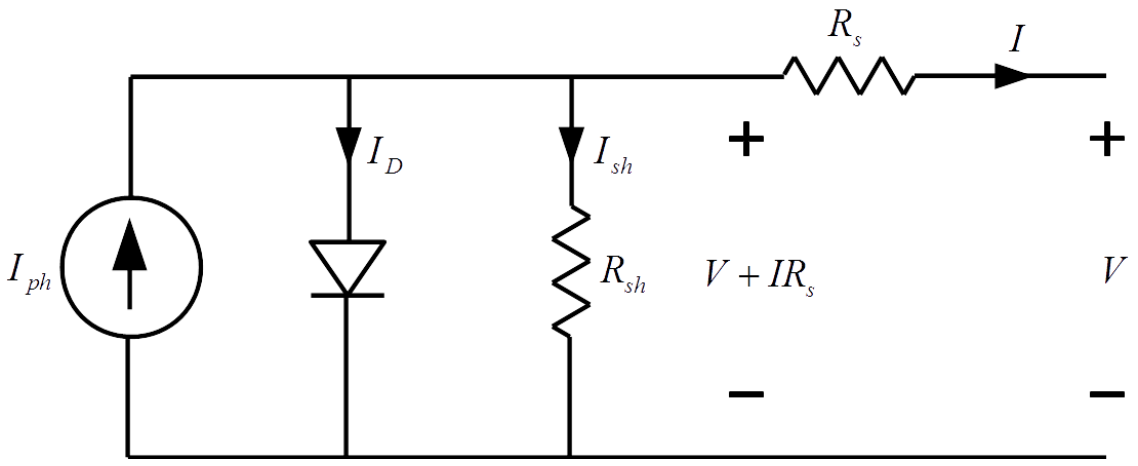

Figure 5: Single diode equivalent circuit

3.0 RESULTS

The graphs of power versus time and series resistance versus time are shown in Figure 6 and Figure 7 respectively. The total energy yield from solar panels with Sn-Ag-Cu solder and Sn-Ag-Cu-Pt solder are 0.4143kWh and 0.4544kWh respectively, i.e., there is an increase of 9.68% when the Sn-Ag-Cu-Pt solder was used as interconnection material. The peak power outputs for the solar panels (Figure 8) are: 15.21W – 18.28W for the Sn-Ag-Cu interconnection and 17.97W – 19.29W for the Sn-Ag-Cu-Pt interconnection. Therefore, there is no significant decrease observed in the peak power output. In addition, average series resistances were calculated to be 13.388mΩ and 10.740mΩ for solar panels with Sn-Ag-Cu interconnection and Sn-Ag-Cu-Pt interconnection respectively. Since both solar panels were manufactured using identical process and materials except for different solder as interconnection materials, the decrease in solder resistance equals to the decrease in series resistance, or 19.78%.

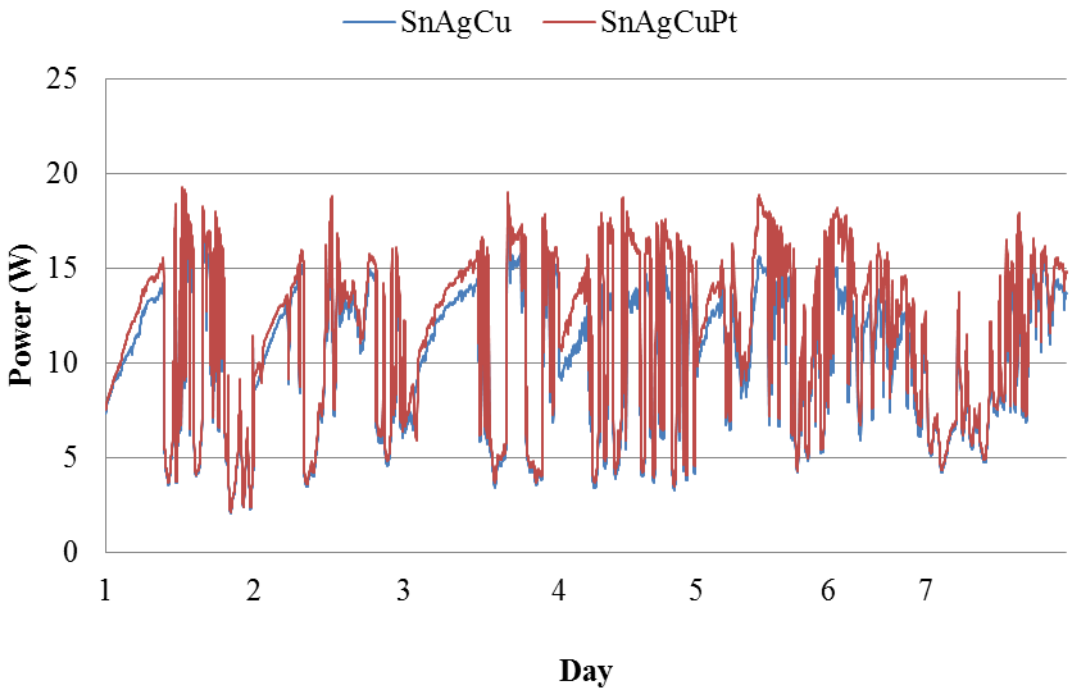

Figure 6: Power output of both solar panels versus time

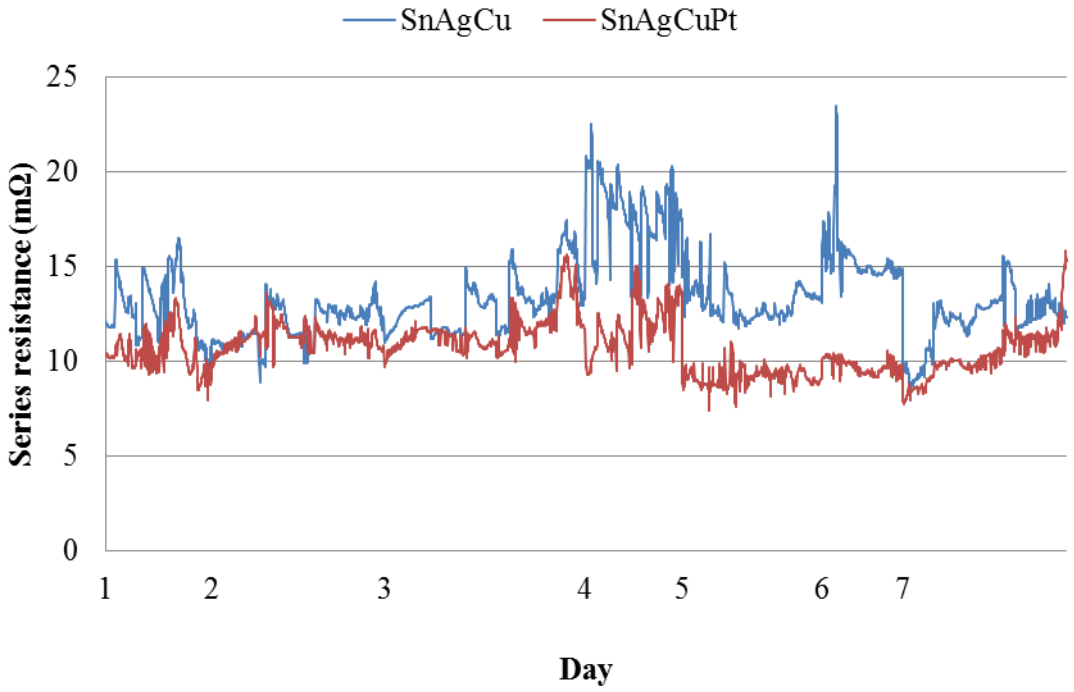

Figure 7: Series resistance of both solar panels versus time

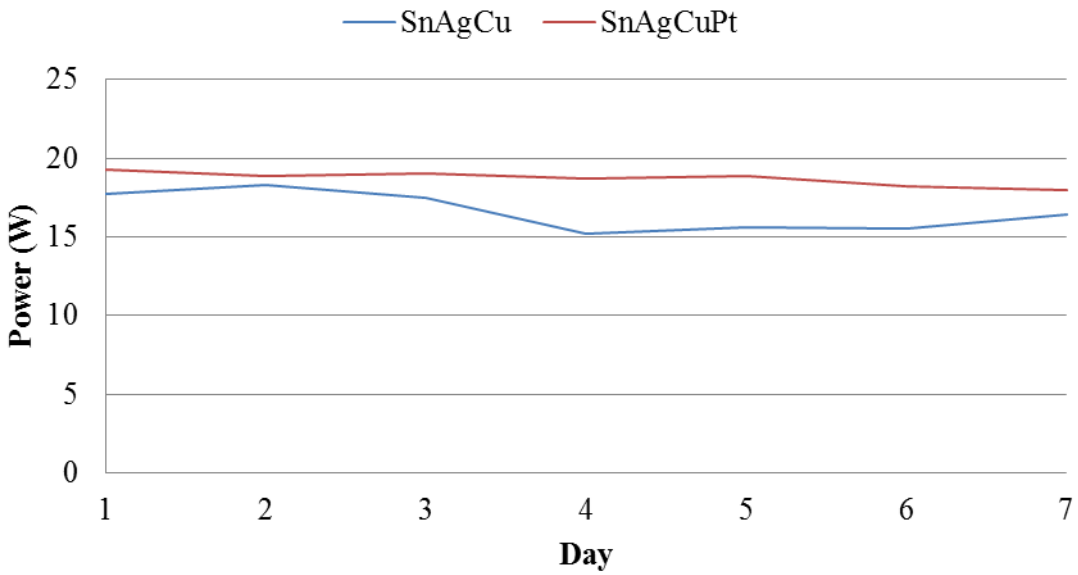

Figure 8: Peak power output throughout the experiment

The percentage of increase in daily energy yield and percentage of decrease in solder resistance are shown in Figure 9. A correlation was found between these percentages, (Figure 10), implying that the reduction in solder resistance results in the output of more energy in a day from the solar panel.

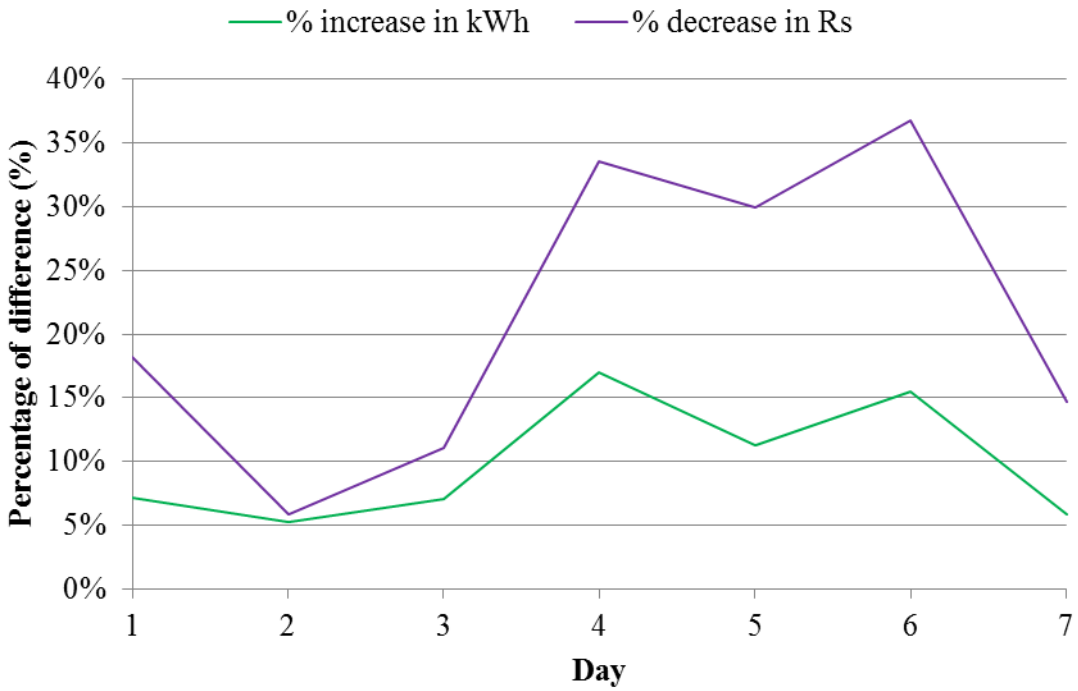

Figure 9: Percentage of increase in daily energy yield and percentage of decrease in solder resistance

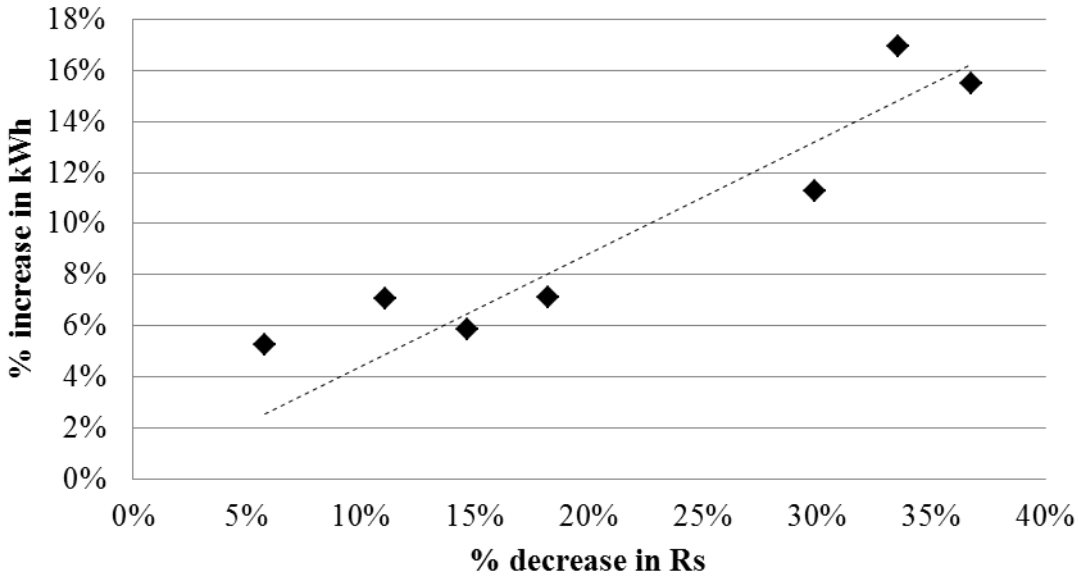

Figure 10: Correlation between the percentages of decrease in solder resistance and the percentage of increase in energy yield

The decrease in solder joint resistance by adding Pt into the Sn-Ag-Cu solder can be explained by comparing the cross-sectional microstructures for both the Sn-Ag-Cu and Sn-Ag-Cu-Pt interconnections (Figure 11 & Figure 12). In both solder joints, Cu_6Sn_5 intermetallic compound (IMC) layer formed at the solder-copper ribbon interface while Ag_3Sn IMC layer formed at the solder- silver metallization interface.

At the Sn-Ag-Cu solder- copper ribbon interface, scallop-shaped Cu_6Sn_5 IMCs makes up the IMC layer with several large and spiky IMCs on the layer; and block-like Ag_3Sn IMCs with sharp edges formed at the Sn-Ag-Cu solder- silver metallization interface. These sharp-edged IMCs are local stress concentrators which will initiate crack propagation in the solder joint and eventually affect the solder joint reliability. The voids present at the solder-silver metallization interface disrupt the electrical current flow and causes the increase in resistance of the solder joint.

In the Sn-Ag-Cu-Pt solder joint (Figure 12), scallop-shaped Cu_6Sn_5 IMCs were evenly distributed along the solder-copper ribbon interface and larger, block-like Ag_3Sn IMCs were formed at the solder- silver metallization interface. With the presence of 0.20 wt.% of Pt in the Sn-Ag-Cu solder, the interfacial morphology of solder joint was altered through formation of an even, continuous IMC layer and reduction in the number of voids. This accounts for the reduction of electrical resistance, hence the increase in the power output of the solar panel.

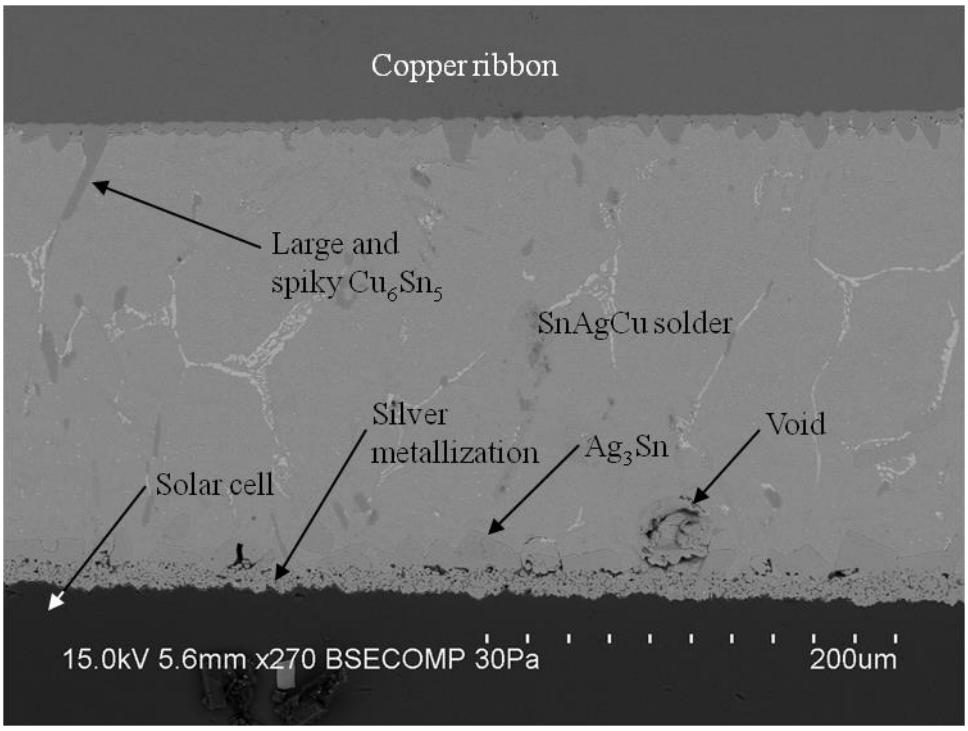

Figure 11: Micrograph of the Sn-Ag-Cu solder joint

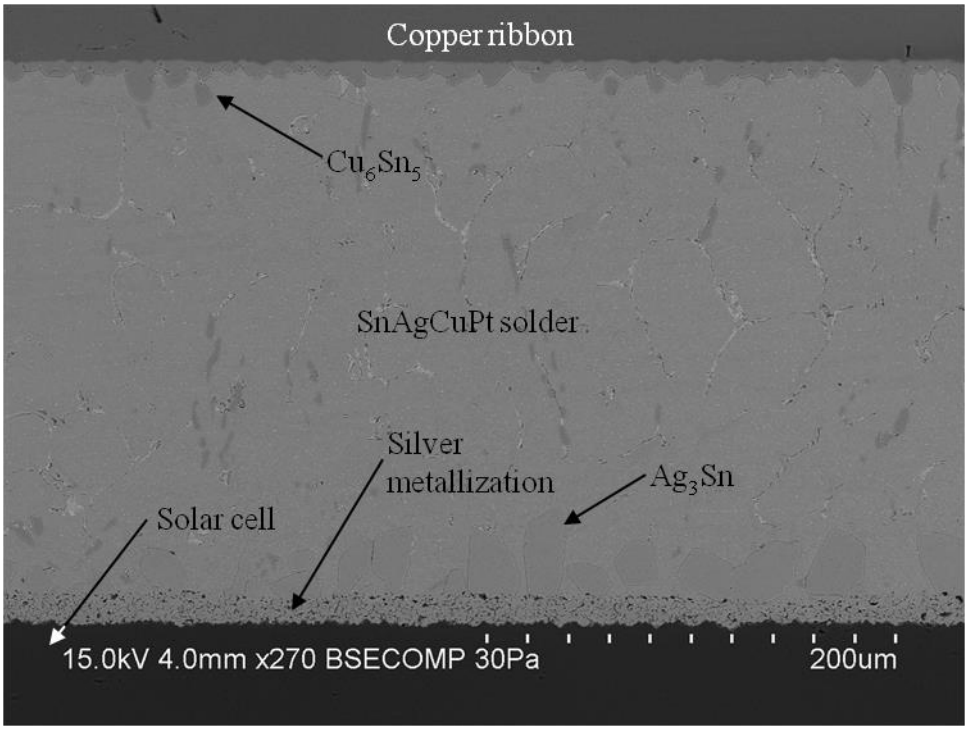

Figure 12: Micrograph of the Sn-Ag-Cu-Pt solder joint

4.0 CONCLUSIONS

The novel Sn-Ag-Cu-Pt solder improved the bi-facial solar panel performance: total energy yield was increased by 9.68%. The increase in the solar panel yield energy is due to the reduction in solder resistance by 19.78%. Peak power outputs from the solar panels throughout a day were almost constant throughout the period of measurement, indicating that the novel Sn-Ag-Cu-Pt solder does not show any sign of degradation under the sun.

REFERENCES

1. P. Schmitt, P. Kaiser, C. Savio, M. Tranitz, U. Eitner. Intermetallic Phase Growth and Reliability of Sn-Ag-Soldered Solar Cell Joints. Energy Procedia 2012, (27):664–669.
2. L. Quan, D. Frear, D. Grivas, J.W. Morris. Tensile behavior of pb-sn solder/cu joints. JEM 1987, (16):203–208.
3. M. Cole, T. Caulfield. Constant strain rate tensile properties of various lead based solder alloys at 0, 50, and 100° C. Scripta metallurgica et materialia 1992, (27):903–908.
4. H.L. Reynolds, J.W. Morris. The role of Cu-Sn intermetallics in wettability degradation. JEM 1995, (24):1429–1434.
5. D.R. Frear, P.T. Vianco. Intermetallic growth and mechanical behavior of low and high melting temperature solder alloys. MMTA 1994, (25):1509–1523.
6. H.H.Hsieh, F.M.Lin, S.P.Yu. Performance of low series-resistance interconnections on the polycrystalline solar cells. Solar Energy Materials and Solar Cells 2011, (95):39–44.
7. S. Ransome, J. Wohlgemuth In: Proceedings of 3rd World Conference on Photovoltaic Energy Conversion, 2003. p. 2206–2209.
8. K.N.Tu, K. Zeng. Tin–lead (SnPb) solder reaction in flip chip technology. Materials Science and Engineering: R: Reports 2001, (34):1–58.
9. A.F. Skipor, S.V. Harren, J. Botsis. The effect of mechanical constraint on the flow and fracture of 63/37 Sn/Pb eutectic alloy. Engineering Fracture Mechanics 1995, (52):647–669.
10. Y. Qi, H.R. Ghorbani, J.K. Spelt. Thermal Fatigue of SnPb and SAC Resistor Joints: Analysis of Stress-Strain as a Function of Cycle Parameters. IEEE Transactions on Advanced Packaging 2006, (29):690–700.
11. C. Melton In: Proceedings of the 1993 IEEE International Symposium on Electronics and the Environment, 1993. p. 94–97.
12. M. Abtew, G. Selvaduray. Lead-free Solders in Microelectronics. Materials Science and Engineering: R: Reports 2000, (27):95–141.
13. E.P. Wood, K.L. Nimmo. In search of new lead-free electronic solders. JEM 1994, (23):709–713.

14. C.M.L. Wu, D.Q. Yu, C.M.T. Law, L. Wang. Microstructure and mechanical properties of new lead-free Sn-Cu-RE solder alloys. Journal of Elec Materi 2002, (31):928–932.
15. C.M. Miller, I.E. Anderson, J.F. Smith. A viable tin-lead solder substitute: Sn-Ag-Cu. JEM 1994, (23):595–601.
16. M.E. Loomans, M.E. Fine. Tin-silver-copper eutectic temperature and composition. Metall and Mat Trans A 2000, (31):1155–1162.
17. K.-W. Moon, W.J. Boettinger, U.R. Kattner, F.S. Biancaniello, C.A. Handwerker. Experimental and thermodynamic assessment of Sn-Ag-Cu solder alloys. Journal of Elec Materi 2000, (29):1122–1136.
18. O.M. Abdelhadi, L. Ladani. IMC growth of Sn-3.5Ag/Cu system: Combined chemical reaction and diffusion mechanisms. Journal of Alloys and Compounds 2012, (537):87–99.
19. F. Lin, W. Bi, G. Ju, W. Wang, X. Wei. Evolution of Ag3Sn at Sn–3.0Ag–0.3Cu–0.05Cr/Cu joint interfaces during thermal aging. Journal of Alloys and Compounds 2011, (509):6666–6672.
20. W.G. Bader. Dissolution of Au, Ag, Pd, Pt, Cu and Ni in a molten tin-lead solder. Weld. J. 1969.
21. J.. Kuhmann, C.-H. Chiang, P. Harde, F. Reier, W. Oesterle, I. Urban, A. Klein. Pt thin-film metallization for FC-bonding using SnPb60/40 solder bump metallurgy. Materials Science and Engineering: A 1998, (242):22–25.